⌘ *Author's Choice*

THE JOURNAL OF BIOLOGICAL CHEMISTRY VOL. 285, NO. 53, pp. 41724–41731, December 31, 2010


# Functional Dissection of Adenylate Cyclase R, an Inducer of Spore Encapsulation*[S]

Received for publication, June 20, 2010, and in revised form, September 26, 2010 Published, JBC Papers in Press, October 21, 2010, DOI 10.1074/jbc.M110.156380

**Zhi-hui Chen, Christina Schilde, and Pauline Schaap**[1]

*From the College of Life Sciences, University of Dundee, Dundee DD15EH, Scotland, United Kingdom*

**Cyclic AMP acting on protein kinase A controls sporulation and encystation in social and solitary amoebas. In *Dictyostelium discoideum*, adenylate cyclase R (ACR), is essential for spore encapsulation. In addition to its cyclase (AC) domain, ACR harbors seven transmembrane helices, a histidine kinase domain, and two receiver domains. We investigated the role of these domains in the regulation of AC activity. Expression of an ACR-YFP fusion protein in *acr*$^-$ cells rescued their sporulation defective phenotype and revealed that ACR is associated with the nuclear envelope and endoplasmic reticulum. Loss of the transmembrane helices (ΔTM) caused a 60% reduction of AC activity, but ΔTM-ACR still rescued the *acr*$^-$ phenotype. The isolated AC domain was properly expressed but inactive. Mutation of three essential ATP-binding residues in the histidine kinase domain did not affect the AC activity or phenotypic rescue. Mutation of the essential phosphoryl-accepting aspartate in receivers 1, 2, or both had only modest effects on AC activity and did not affect phenotypic rescue, indicating that AC activity is not critically regulated by phosphorelay. Remarkably, the dimerizing histidine phosphoacceptor subdomain, which in ACR lacks the canonical histidine for autophosphorylation, was essential for AC activity. Transformation of wild-type cells with an ACR allele (ΔCRA) that is truncated after this domain inhibited AC activity of endogenous ACR and replicated the *acr*$^-$ phenotype. Combined with the observation that the isolated AC domain was inactive, the dominant-negative effect of ΔCRA strongly suggests that the defunct phosphoacceptor domain acquired a novel role in enforcing dimerization of the AC domain.**

The ATP derivative cAMP is the most deeply conserved signaling intermediate in all domains of life. In eukaryotes, cAMP is produced by the conserved class III cyclase domain, whereas prokaryotes use five more unrelated catalysts. The class III domain can be subdivided into four subtypes, a–d, with type IIId, which is found in fungi and Euglenozoa, being derived from type IIIc, which is common to both bacteria and Archaea (1, 2). Type IIIa is the predominant catalyst in metazoa but is also found in protozoa and prokaryotes. In metazoa, it is present as two asymmetrical copies alternating with two sets of six transmembrane (TM)[2] helices in the G-protein-regulated adenylate cyclases and as a single copy in the guanylyl cyclases. Type IIIb domains are very abundant in prokaryotes, where they are typically combined with many other functional domains but are also found in alveolates, Amoebozoa, and mammals. Some of the alveolate enzymes harbor an additional set of six TM helices, whereas others and the mammalian enzyme are soluble proteins (3, 4). The amoebozoan adenylate cyclase ACR from the social amoeba *Dictyostelium discoideum* is a multidomain protein, which resembles some of the cyanobacterial type IIIb enzymes with respect to domain architecture (5, 6).

Social amoebas use cAMP not only as a second messenger for external stimuli but also as a secreted primary signal. In this role, cAMP coordinates the aggregation of starving amoeba and the construction of fruiting bodies, and it also triggers the expression of aggregation genes and prespore genes. As second messenger, cAMP mediates the effect of a range of stimuli that control initiation of multicellular development, maturation of stalk and spore cells, and germination of the spores (7, 8). Comparative analysis of cAMP signaling throughout the social amoebas showed that the roles of cAMP in spore formation and germination are evolutionary derived from a deeply conserved role in the encystation of solitary amoebas (2, 9). Encystation is of considerable medical relevance because cysts are resistant to biocides and immune clearance and preclude effective treatment of diseases by protozoan pathogens (10–12). The mechanisms of encystation are little understood, and an understanding of the role of cAMP in this process will have important therapeutic consequences.

The type IIIb enzyme ACR/ACB (5, 6) is essential for spore maturation and proper stalk cell formation in *D. discoideum*, which additionally uses two type IIIa enzymes: adenylate cyclase A and adenylate cyclase G. Adenylate cyclase A mainly produces cAMP for secretion and coordination of cell movement (13, 14), whereas adenylate cyclase G is required for prespore differentiation and control of spore dormancy (15, 16). ACR is a large multidomain protein in which the cyclase catalytic domain is preceded by two receiver domains, a histine kinase region, consisting of a HisKA (histidine kinase phosphoacceptor domain) and HATPase (histidine kinase-, DNA gyrase B-, and phytochrome-like ATPases) C domain and seven TM helices (6). ACR activity is present during growth,

* This work was supported by Wellcome Trust Grant 076618 (to P. S.).
⌘ *Author's Choice*—Final version full access.
[S] The on-line version of this article (available at http://www.jbc.org) contains supplemental Table S1, Fig. S1, and additional references.
[1] To whom correspondence should be addressed: MSI/WTB/JBC Complex, Dow St., Dundee DD15EH, Scotland, United Kingdom. Fax: 44-1382-345386; E-mail: p.schaap@dundee.ac.uk.

[2] The abbreviations used are: TM, transmembrane; AC, adenylate cyclase; R, receiver/response regulator; YFP, yellow fluorescent protein; f, forward; r, reverse.

decreases during aggregation, and increases again after aggregation to reach maximum levels during fruiting body formation (17).

Until now, it was not known whether and how the histidine kinase and receiver domains of ACR regulate its cyclase activity. More information is available on the type IIIb cyclase CyaC from the cyanobacterium *Spirulina platensis*. Like ACR, CyaC also contains a histidine kinase and receiver domain proximal to the carboxyl-terminal AC domain but additionally contains two, more distal GAF (found in cGMP-phosphodiesterases, adenylyl cyclases and formate hydrogen lyase transcriptional activator) domains and a second N-terminal receiver domain. Here, cyclase activity is activated by phosphorylation of the proximal receiver domain by the intrinsic histidine kinase activity (18). In another cyanobacterium, *Anabaena* sp., cyclase activity is up-regulated by phosphorylation of the N-terminal receiver domain in response to far-red light via the phytochrome-like sensor histidine kinase AphC (19). In theory, ACR could also be regulated by any of the 15-sensor histidine kinases that are present in *Dictyostelium* (20).

In this work, we investigated the cellular localization of ACR and the role of its multiple functional domains in the control of AC activity. Our data show a novel role for the HisKA domain in dimerization of the cyclase domain and unusual localization of the enzyme at the cell nucleus.

## EXPERIMENTAL PROCEDURES

*Cell Lines and Culture*—*D. discoideum* NC4A2 (21) and *acr*$^-$ cells (see below) were cultured in HL5 medium that was supplemented with 5 $\mu$g/ml blasticidin for null mutants and with 10 to 100 $\mu$g/ml G418 for cells harboring expression constructs. *D. discoideum* NC4 was grown in association with *Klebsiella aerogenes* on standard medium agar. Multicellular development was induced by incubating cells, freed from bacteria or growth medium, at 22 °C on phosphate buffered agar (1.5% agar in 10 mM sodium/potassium phosphate buffer, pH 6.5) at $1.5 \times 10^6$ cells/cm$^2$.

*Gene Disruption*—To generate an *AcrA* knock-out construct with recyclable selection marker, nucleotides 350–1382 (KO1) and nucleotides 1638–2685 (KO2) of the *AcrA*-coding region were amplified by PCR from AX2 genomic DNA with primer pairs KO1f/KO1r and KO2f/KO2r, that harbor a KpnI/SalI and BamHI/NotI restriction site, respectively (supplemental Table S1). The KO1 and KO2 fragments were inserted by T/A cloning into vector pCR4-TOPO (Invitrogen), released by KpnI/SalI or BamHI/NotI digestion, and cloned into KpnI/SalI and BamHI/NotI sites that flank the floxed A15::Bsr selection cassette of vector pLPBLP (22) generating pACR-KO (supplemental Fig. S1*A*). NC4A2 cells were transformed with pACR-KO KpnI/NotI insert by electroporation, selected for growth at 5 $\mu$g/ml blasticidin, and cloned out on *Klebsiella aerogenes* lawns. Clonal isolates were tested for gene disruption by two PCR reactions using primer pairs KO1f/KOt1 and BsrF/KOt2 (supplemental Table S1 and Fig. S1*A*) and examination of genomic digests by Southern blot.

*ACR Expression Construct*—The complete 6372-nucleotide *ACR* cDNA was cloned by a stepwise approach in which the sequence was divided into four segments, which were amplified and assembled sequentially. The first segment AB (containing the single intron position of *ACR*) was amplified with primers A and B (supplemental Table S1) by reverse transcription PCR of mRNA isolated from 12 h-starved AX2 cells. Segments CD, EF, and GH were all amplified from AX2 genomic DNA by PCR using primer sets C/D, E/F, and G/H for the three segments, respectively (supplemental Table S1). The primers contained restriction sites that were either already present in the *ACR* sequence or were introduced by neutral mutations. The four segments were individually cloned into pCR4-TOPO, sequenced to validate correct amplification, and released by their respective pairs of restriction enzymes. The segments were then inserted into pGEM-7Zf(+) (Promega, Madison, WI) step by step at their corresponding restriction sites, as outlined in supplemental Fig. S1*B*. Next, the full-length *ACR* cDNA was excised with BamHI and XhoI and inserted into the BamHI/XhoI-digested expression vector pB17S-EYFP. This places *ACR* under control of the constitutively active A15 promoter and fuses the gene at the C terminus to an enhanced yellow fluorescent protein (YFP) tag (23).

*ACR Deletion Constructs*—The truncated forms were created by replacing one or several of the four *ACR* segments (supplemental Fig. S1*B*) in pGEM-7Zf(+) with a newly amplified truncated version of the relevant region, using a combination of primers ΔT, ΔTK, ΔTKC, ΔTKCR1, and ΔTKCR1R2 (supplemental Table S1) that incorporate a 5′-BamHI site, with reverse primers D or F (supplemental Table S1) for N-terminal truncations, and primer ΔC, with a XhoI site, combined with forward primer G for the C-terminal truncations. The complete truncated *ACR* cDNA was released from pGEM-7Zf(+) by BamHI/XhoI digestion and inserted into pB17S-EYFP as described above. For the ΔTΔC and ΔTKCR1ΔC double truncations, the ΔT-D and ΔTKCR1-F amplicons were combined with the ΔC construct. The full-length and truncated ACR constructs were transformed into *acr*$^-$ cells by electroporation. Transformants were selected at 10 $\mu$g/ml G418, which was gradually increased to 100 $\mu$g/ml.

Putative dominant-negative fragments were amplified from *ACR* cDNA using forward primer A and reverse primers ΔCRA and ΔKCRA (supplemental Table S1). After subcloning in pCR4-TOPO, the fragments were inserted into pB17S-EYFP using their BamHI/XhoI restriction sites as described above. Both constructs and empty pB17S-EYFP vector were transformed into wild-type NC4A2 cells, with G418 selection increased to 300 $\mu$g/ml.

*Site-directed Mutagenesis*—Single or multiple amino acid mutations were introduced by amplifying the entire pCR4-TOPO vector containing the relevant segment of *ACR* with a mutagenic forward (f) and reverse (r) primer pair. The mutations H613Q, S617A, and S617E of the HRRLS motif in segment AB were performed with primer pairs H613Qf/H613Qr, S617Af/S617Ar and S617Ef/S617Er (supplemental Table S1), respectively. The mutation of three residues in the HATPase-C domain, N769D, D854A, and G856A, were achieved by two PCR reactions with primer pairs N769Df/N769Dr and D854AG856Af/D854AG856Ar on segment CD. Mutations

D1010A in the R1 domain and D1089A in the R2 domains were obtained by amplification of segments CD and EF, respectively, with primer pairs D1010Af/D1010Ar and D1089Af/D1089Ar. All mutated segments were validated by DNA sequencing, excised from pCR4-TOPO by their terminal restriction sites, and recombined with the complementary intact ACR segments in pGEM-7ZF(+) to reconstitute the full-length ACR cDNA, as described above. A double D1010A/D1089A mutant was obtained by combining the mutated CD and EF segments with wild-type AB and GH segments (supplemental Fig. S1*B*). The mutant *ACR* cDNAs were then inserted into pB17S-EYFP and transformed into *acr*$^-$ cells.

*Adenylyl Cyclase Activity Measurement in Cell Lysates*—Cells transformed with intact or mutant ACR-YFP constructs were harvested during exponential growth, washed once with PB (10 mM sodium/potassium phosphate buffer, pH 6.5) and resuspended in lysis buffer (2 mM $MgCl_2$ and 250 mM sucrose in 10 mM Tris, pH 8.0) to $10^8$ cells/ml. Cells were lysed by passage through 3-$\mu$m pore size nuclepore filters. Aliquots of 10 $\mu$l cell lysate were added to 10 $\mu$l of 2× assay mix (1 mM ATP, 16 mM $MgCl_2$, 0.4 mM 3-isobutyl-1-methylxanthine, and 20 mM dithiothreitol in lysis buffer). After 5 min of incubation on ice, reactions were started by transferring the samples to a 22 °C water bath. Reactions were terminated after 0, 3, 10, 20, and 30 min by adding 10 $\mu$l of 0.4 M EDTA (pH 8.0), followed by boiling for 1 min. cAMP was assayed directly in the boiled lysate by isotope dilution assay (17). AC activities were standardized on the amount of YFP tag in the lysates, determined by quantitative Western blot analysis.

*Qualitative and Quantitative Western Blot Analysis*—Cells were harvested and lysed in SDS-PAGE sample buffer, or filter-lysed cells were mixed with sample buffer. Proteins were size-fractionated by SDS-PAGE, transferred to nitrocellulose, and probed with rabbit polyclonal αGFP antibodies (Abcam, Cambridge, UK) For qualitative analysis, blots were incubated with horseradish peroxidase conjugated goat anti-rabbit secondary antibody (Sigma), and detection was performed with the SuperSignal chemoluminescence kit (Pierce). For quantitative analysis, the secondary antibody was IR dye 800-conjugated donkey anti-rabbit antibody (Invitrogen), and signal intensities were analyzed using the Odyssey infrared imaging system (LI-COR, Lincoln, NE).

*Immunofluorescence*—Cells were washed with phosphate buffer, left to adhere to coverslips, and fixed with 15% picric acid/paraformaldehyde. Cells were post-fixed with 70% ethanol, washed with PBS (24), and were incubated overnight at 8 °C with a polyclonal rabbit anti-GFP antibody (Abcam), diluted 1:100 in PBSB (1% bovine serum albumin in PBS), and 1:100 diluted monoclonal mouse anti-calnexin antibody (24) to detect ACR-YFP and calnexin, respectively. After three washes with PBS, the cells were incubated for 2 h at 22 °C with 1:100 diluted FITC-conjugated donkey anti-rabbit IgG (Diagnostics Scotland, Edinburgh, Scotland) and 1:500 diluted Alexa Fluor® 594 conjugated goat anti-mouse IgG (Invitrogen) to detect the α-GFP and α-calnexin antibodies, respectively, and simultaneously counterstained with 0.1 $\mu$g/ml of the DNA stain DAPI (Invitrogen). Coverslips were washed three times in PBS and mounted to slide glasses with Hydromount (National Diagnostics).

## RESULTS

*Bioinformatics*—To gain initial insight in the functionality of the putative regulatory domains of ACR, we compared their sequences with those of structurally resolved homologous domains. Histidine kinases consist of an HisKA-dimerizing domain that also carries the histidine for autophosphorylation and an ATP binding HATPase-C (HisC) domain.

The HisKA domain contains two α-helices, which form an intramolecular dimer with a second HisKA domain, creating a four-helix bundle. Dimerization enables trans-phosphorylation by the HisC domain of two His residues that point outward from two of the four helices. The phosphoryl group is subsequently transferred to the Asp of a receiver (R) domain. The HisKA domain in conjunction with the HisC domain can also act as an R domain-directed phosphatase (25, 26).

The ACR HisKA domain contains two adjacent α-helices but lacks the conserved His and other residues that are essential for both autokinase and phosphatase activity (Fig. 1*A*). Between helix I and the seventh TM domain, ACR harbors another predicted α-helix that contains an HRRLS motif. Apart from a putative His phosphoryl-acceptor, this motif also contains a consensus protein kinase A phosphorylation site (RR*x*S) (27).

The HisC domain is characterized by five conserved sequence motifs (N, G1, F, G2, and G3) that line the ATP-binding pocket (28). Alignment of the HisC domain of ACR with structurally resolved HisC domains shows that the residues that define the five motifs are conserved (Fig. 1*B*). Mutagenesis of the bacterial enzyme CheA showed that residue $Asn^{409}$ that marks the N motif, residues $Asp^{449}$ and $Gly^{451}$ in the G1 motif, and $Gly^{502}$ in the G2 motif are essential for its kinase activity (29, 30). For EnvZ, which, unlike CheA, can also act as a receiver-directed phosphatase, mutation of $Asn^{347}$ (equivalent to $Asn^{409}$) and $Asn^{343}$ in the N motif, and $Phe^{390}$ in the F motif (*green* highlights) leads to loss of kinase, but not phosphatase activity, whereas mutation of $Thr^{402}$ in the G2 box (*pink* highlight) has the opposite effect (25, 31). However, most residues required for phosphatase activity reside in the HisKA domain (Fig. 1*A*). All essential residues for kinase activity are present in ACR, suggesting that its HisC domain could be functional. The ACR HisC domain is however anomalous in harboring a 51-amino acid insertion of low complexity sequence in the first β-sheet.

R domains catalyze transfer of a phosphoryl group from a HisKA domain to one of their own Asp residues. They regulate the activities of associated effectors and catalyze autodephosphorylation. Phosphorylation requires association with a $Mg^{2+}$ ion that is positioned in the conserved active site and commonly causes movement of a conserved Thr or Ser and Tyr or Phe switch residue pair toward the active site. This conformational change then regulates effector activity (28, 32). Alignment of the ACR R domains with two well characterized R domains shows that both the secondary structure elements and the active site residues (*bold/underlined*) are conserved in ACR_R1 (Fig. 1*C*). ACR_R2 lacks two of four

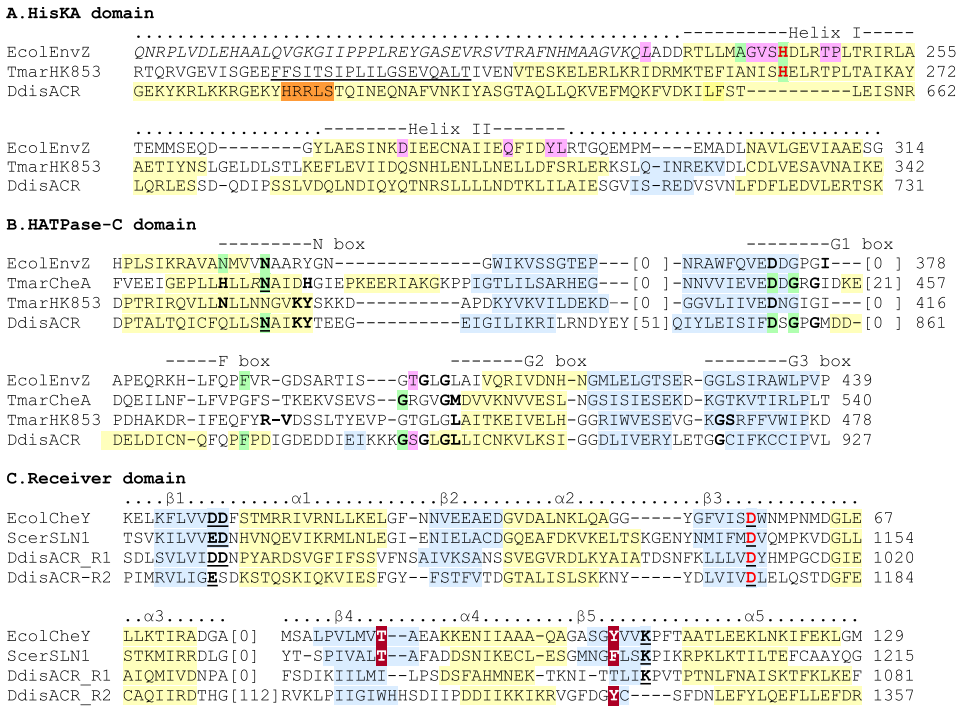


FIGURE 1. **Alignment of ACR functional domains with structurally resolved homologous domains.** The location of α-helices (*yellow*) and β-sheets (*blue* highlight) were retrieved from the NCBI Molecular Modeling Database entries for all structurally resolved structures or predicted using PSIPRED (41) for the ACR domains. *Green*, essential for autokinase activity in CheA (29, 30) and for autokinase but not receiver-directed phosphatase activity in EnvZ; *pink*, essential for receiver-directed phosphatase but not autokinase activity in EnvZ (25, 31). *A*, HisKA domain. The ACR HisKA domain and flanking sequence from the seventh TM domain up to the HisC domain were aligned with the HisKA domains and corresponding regions of EcolEnvZ and TmarHK853 (42, 43). *Red text*, phosphoryl-accepting histidine. *Orange*, HRRLS motif. *Italic letters*, HAMP domain; *underlined letters*, TM domain. Protein Data Bank codes are as follows: 1JOY, EcolEnvZ; 2C2A, TmarHK953. *B*, HATPase-C domain. The ACR HisC domain was aligned with three structurally resolved bacterial HisC domains. Residues in *boldface type* represent those demonstrated to interact with ATP (43–46); *bold/underlined* residues are those that interact with $Mg^{2+}$ (45). When functionally essential residues are conserved in ACR, they are similarly marked. Protein Data Bank codes are as follows: 1BXD, EcolEnvZ; 1I59, TMarCheA; 2C2A, TmarHK853. *C*, receiver domain. The two ACR receiver domains R1 and R2 were aligned with two structurally resolved R domains from yeast and *Escherichia coli*. *Red text*, phosphoryl-accepting aspartate. *Bold/underlined text*, residues in the $Mg^{2+}$-binding active site, *maroon*, switch residues that reorient upon phosphorylation (47–50). Protein Data Bank codes are as follows: 1F4V, EcolCheY; 2R25, ScerSLN1.

active site residues and additionally harbors a 112-amino acid insertion. Neither R1 nor R2 contain a complete Thr/Ser-Tyr/Phe switch residue pair (*maroon* highlight). The phosphoryl-accepting Asp (*red text*) is conserved in both R1 and R2, but their other anomalies may well interfere with domain functionality.

*Expression and Activity of a Full-length ACR-YFP Fusion Protein*—Due to its large size, the 6.4-kb required amplification and cloning ACR cDNA in four segments into pGEM-7Zf(+) followed by subcloning into the extrachromosomal expression vector pB17S-EYFP. In this vector, ACR expression is driven by the constitutive A15 promoter, and the gene is fused at the C terminus to an enhanced YFP tag. The empty vector (YFP) and the ACR-YFP construct were expressed in an *acr*$^-$ mutant. As shown previously (6), *acr*$^-$ cells develop normally up to the fruiting body stage but are then defective in spore encapsulation, whereas they also form stalks that are thinner than those of wild-type cells. Both aspects of the *acr*$^-$ phenotype were restored by transformation with the ACR-YFP construct but not with the empty vector (Fig. 2*A*). Inspection of the cells by confocal microscopy showed that YFP-tagged ACR was associated with the nuclear envelope and a vesicular network throughout the cell (Fig. 2*B*). Incubation of fixed *acr*$^-$/ACR-YFP cells with antibodies raised against GFP/YFP and the endoplasmic reticulum marker calnexin (24) showed colocalization of ACR-YFP and calnexin around the nuclei and the vesicular network (Fig. 3). This strongly suggests that ACR localizes to the endoplasmic reticulum and nuclear envelope. Western blots of fractionated *acr*$^-$/ACR-YFP cell lysates, probed with YFP antibodies, confirmed that ACR-YFP is expressed at the expected size of 270 kDa in the nuclear fraction (Fig. 2*C*). The ΔT ACR-YFP mutant, which lacks the transmembrane domains (Fig. 4) was present predominantly in the cytoplasmic fraction (Fig. 2*C*) and showed a similar localization as YFP alone over the entire cytoplasm of the cell (Fig. 2*B*).

ACR activity can be measured in cell lysates with $Mg^{2+}$-ATP as a substrate and 3-isobutyl-1-methylxanthine and DTT present to inhibit the phosphodiesterases RegA and PdsA, respectively. The other *D. discoideum* adenylate cyclases adenylate cyclase G and adenylate cyclase A are only expressed to low levels in vegetative cells and require $Mn^{2+}$ and/or $Mg^{2+}$ plus GTPγS, respectively, to be assayed in cell lysates (17). Consequently, *acr*$^-$/YFP lysates show very little cAMP accumulation, whereas *acr*$^-$/ACR-YFP lysates produce cAMP at a steady rate of 1.3 pmol/min mg protein (Fig. 2*D*). Combined with its ability to restore the *acr*$^-$ phenotype, these data indicate that the ACR-YFP fusion protein is fully functional.

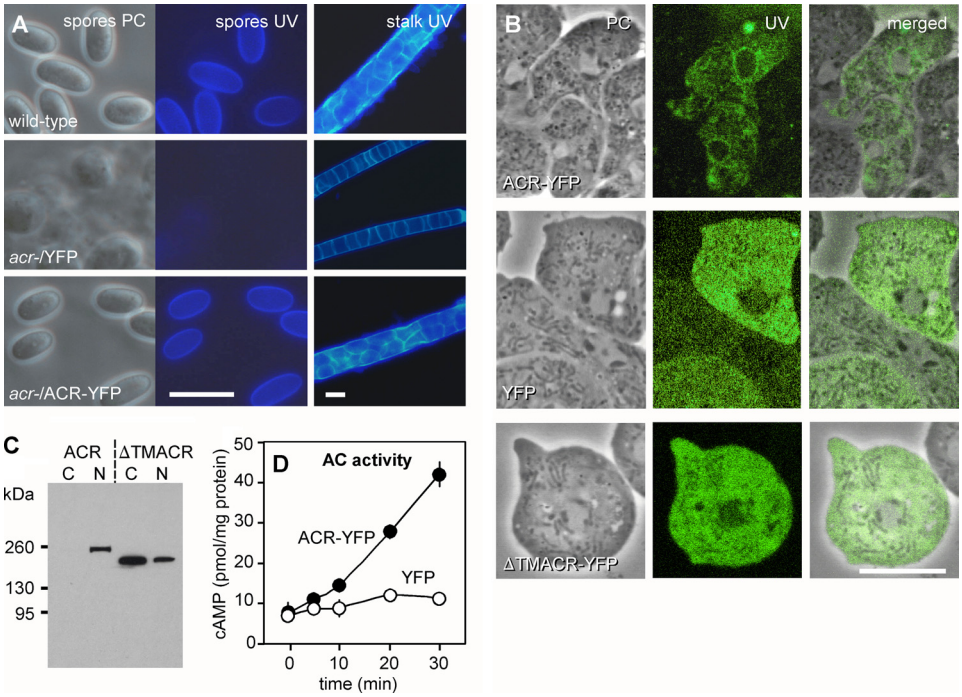


FIGURE 2. **Expression and activity of a full-length ACR construct.** *A*, complementation of acr$^-$. Full-length *ACR* cDNA was cloned into vector pB17S-EYFP in between the constitutive A15 promoter and YFP. This vector was transformed into an *acr*$^-$ mutant to yield *acr*$^-$/ACR-YFP cells. Wild-type, *acr*$^-$*/ACR-YFP*, and *acr*$^-$ cells transformed with empty vector (*acr*$^-$*/YFP*) were starved on PB agar until fruiting bodies had formed, which were transferred to a droplet of PB with 0.01% Calcofluor on a glass slide and photographed using a Leica DMLB2 fluorescence microscope under phase contrast (*PC*) and UV illumination. *B*, cellular localization of ACR. Phase contrast images and optical sections of YFP fluorescence in living *acr*$^-$*/ACR-YFP*, *acr*$^-$*/YFP* and *acr*$^-$*/ΔTMACR-YFP* cells were obtained with a Leica DMRBE confocal laser scanning microscope. *C*, cell fractionation. Vegetative *acr*$^-$*/ACR-YFP* and *acr*$^-$*/ΔTMACR-YFP* cells were lysed through nuclepore filters. Lysates were fractionated by differential centrifugation into cytoplasm (*C*) and nuclei (*N*) as described previously (51), and both fractions were subjected to qualitative Western blotting with α-GFP antibodies. *D*, cAMP production by ACR. Vegetative *acr*$^-$*/ACR-YFP* and *acr*$^-$*/YFP* cells were filter-lysed and incubated for 30 min at 22 °C with AC assay mix (see "Experimental Procedures"). cAMP accumulation was assayed at the indicated time periods and standardized on the protein content of the cell lysates. Means and S.D. of four experiments performed in triplicate are presented. *Scale bars* in *A* and *B*, 10 μm.

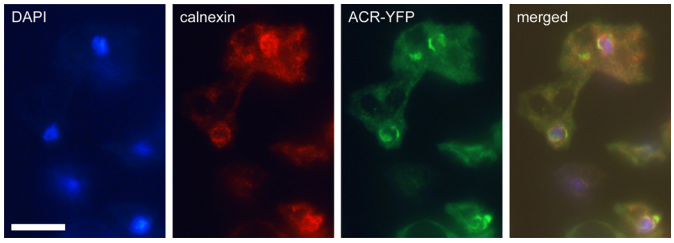


FIGURE 3. **Visualization of ACR-YFP and calnexin by immunofluorescence.** Axenically grown *acr*$^-$/ACR-YFP cells were harvested in exponential phase and triple stained with (i) a polyclonal rabbit-anti-GFP antibody, followed by FITC conjugated donkey anti-rabbit IgG; (ii) a monoclonal mouse-anti-calnexin antibody (24) followed by Alexa Fluor® 594 conjugated goat anti-mouse IgG; and (iii) DAPI to detect ACR-YFP, calnexin, and DNA, respectively. Cells were photographed through the UV, TRITC, and FITC filter sets of a Leica DMLB2 fluorescence microscope. The merged image was prepared with the Qcapture Pro camera software. *Scale bar*, 10 μm.

*Role of ACR Functional Domains in Controlling Cyclase Activity*—We next analyzed the contribution of the different domains of ACR to the regulation of its ability to synthesize cAMP. A range of ACR-YFP fusion constructs was prepared with progressive N- and C-terminal truncations toward the AC catalytic domain (Fig. 4*A*) and expressed in *acr*$^-$ cells. Western blots of cell lysates probed with YFP antibody showed that all constructs produced proteins of the expected size, although absolute expression levels could vary up to 5-fold between constructs (Fig. 4*D*). All cyclase assays were therefore standardized on the amount of YFP in the cell lysates determined by quantitative Western blot analysis. Fig. 4*B* summarizes the activities measured in all constructs, relative to full-length ACR. Truncation of the C-terminal low complexity region induced a 60% increase in ACR activity, both in an otherwise intact construct (ΔL), or combined with the ΔT truncation (ΔTΔL). Loss of all transmembrane domains (ΔT and ΔTΔL) reduced ACR activity by 60%. Additional loss of the HisKA domain (ΔTK) led to almost complete loss of ACR activity. Constructs that additionally lack the HisC (ΔTKC), the R1 domain and the low complexity region (ΔTKCR1ΔL) and both the R1 and R2 domains (ΔTKCR1R2) also show no significant ACR activity. The constructs were also tested for their ability to complement the defect of *acr*$^-$ cells in spore encapsulation and robust stalk formation. Both of these abilities were lost when their AC activity fell below 20% of that of full-length ACR (Fig. 4*C*).

To summarize, it appears that the transmembrane domains contribute to full ACR activity, whereas the HisKA domain is essential for activity. The roles of the HisC, R1, and R2 domains are not resolved. The C-terminal low complexity region is detrimental to full activity. This region predominantly consists of polyglutamine tracts that are common to *D. discoideum* proteins and may in this case cause some nonspecific obstruction to full enzyme activity.

*Functions of Histidine Kinase and Receiver Domains*—Despite the lack of the consensus His for autophosphorylation,

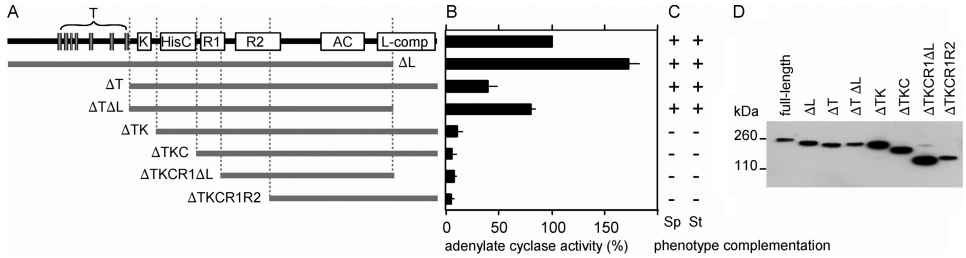


FIGURE 4. **Functions of the different domains of ACR in adenylate cyclase regulation.** *A*, schematic of truncations. Truncated segments of the *ACR* cDNA lacking transmembrane (*T*, *vertical bars*), HisKA (*K*), HisC (*C*), receiver (*R1* and *R2*) domains or the C-terminal low complexity region (*L*) were prepared by PCR amplification and recombined with unaltered segments in pGEM7ZF$^+$ to reconstitute the entire (but truncated) cDNAs, which were then transferred to vector pB17S-EYFP and transformed into *acr*$^-$ cells. *B*, AC activity of truncated proteins. Lysates of transformed cell lines were incubated with AC assay mix for 30 min and assayed for cAMP production. Data are standardized on the amount of YFP fusion protein in the lysates as determined by quantitative Western blotting (see "Experimental Procedures"). The results represent means and S.D. of four experiments performed on cells from at least two separate transformations. *C*, complementation of *acr*$^-$ phenotype. All transformants were developed into fruiting bodies, which were examined as described for Fig. 2*A* for complementation of the spore encapsulation (*Sp*) and thin stalk (*St*) phenotype. *D*, expression levels of truncated proteins. Lysates of $3 \times 10^5$ cells that had been transformed with intact and truncated ACR-YFP fusion constructs were size-fractionated by SDS-PAGE. The YFP-fusion proteins were visualized by qualitative Western blotting using an $\alpha$-GFP antibody.

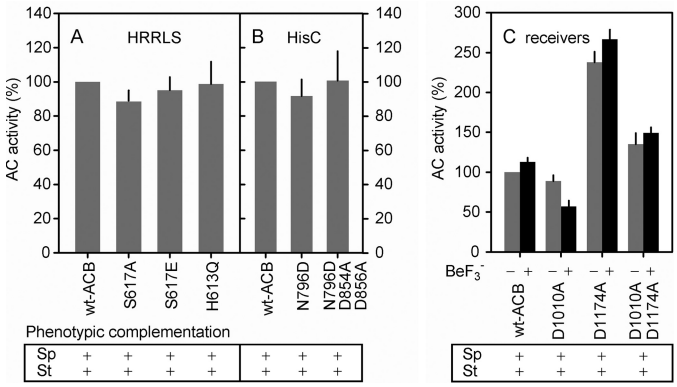


FIGURE 5. **Disruption of domain activity by site-directed mutagenesis.** *A*, putative phosphoryl-accepting residues in the HRRLS motif. His$^{613}$ in the HRRLS motif, which resides in segment AB of ACR (supplemental Fig. S1*B*), was mutated into Gln, whereas Ser$^{617}$ was mutated either into Ala or Glu. The mutated segments were recombined with segments CD, EF, and GH to recreate full-length ACR-YFP, which was transformed into *acr*$^-$ cells and assayed for AC activity as described above. Data are expressed as percentage of AC activity in intact ACR. The transformed *acr*$^-$ cells were additionally developed into fruiting bodies to examine complementation of their spore- and stalk maturation phenotypes by the constructs. *B*, residues essential for histidine kinase activity. Asn$^{769}$ in the HisC domain was first mutated into Asp in segment CD. Later, Glu$^{854}$ and Gly$^{856}$ were both mutated into Ala in segment CD that contained the N769D mutation. The two mutated segments were recombined with segments AB, EF, and GH to recreate full-length ACR-YFP proteins, transformed into *acr*$^-$ cells, and assayed for AC activity and complementation of the *acr*$^-$ phenotype. *C*, receiver domains. The phosphoryl-accepting residues Asp$^{1010}$ in R1 and Asp$^{1174}$ in R2 were mutated into Ala in the individual ACR segments CD and EF, respectively, or in both. The mutated segments were recombined with complementary segments to recreate full-length ACR-YFP and transformed into *acr*$^-$ cells. AC activity was assayed in the presence 5 mM NaF (−) or 5 mM NaF with 0.1 mM $BeCl_2$ to form $BeF_3^-$ (+) (34). Data represent means and S.E. of three experiments performed in triplicate. *Sp*, spore encapsulation; *St*, thin stalk.

the HisKA domain of ACR appears to be essential for its cyclase activity (Fig. 4*B*). ACR harbors an HRRLS motif within an $\alpha$-helix just N-terminal of the HisKA domain, which could be a target for phosphorylation by HisC, protein kinase A, or both (Fig. 1*A*). To test this possibility, we mutated the His$^{613}$ in this motif into Gln, whereas Ser$^{617}$ was mutated both into an inactive Ala and a phosphomimetic Glu. Fig. 5*A* shows that loss of His$^{613}$ had no deleterious effects on ACR activity or complementation of the *acr*$^-$ phenotype and that the modifications of Ser$^{617}$ were equally without significant effects.

To resolve whether the histidine kinase activity of the HisC domain is required for ACR activation, we mutated Asn$^{796}$ in the N box of the HisC domain (Fig. 1*B*), which is essential for ATP binding and catalytic activity, into Asp. Fig. 5*B* shows that this had no effect on ACR activity, and neither had additional mutation of two other essential ATP-binding residues, Asp$^{854}$ and Gly$^{856}$, in the G1 box. This indicates that ACR is not regulated by its intramolecular histidine kinase activity.

To resolve the roles of the two R domains, we mutated the essential phosphoryl-accepting Asp$^{1010}$ and Asp$^{1174}$ in these domains into Ala. Fig. 5*C* shows that the D1010A mutation in R1 caused a 10% reduction of ACR activity, whereas the D1174A mutation in R2 increased ACR activity ~2.5-fold. This was reduced to 1.3-fold when the aspartates in both R domains were mutated into alanines. These data indicate that R1 has a minor stimulatory effect on AC activity, and R2 has a more pronounced, but still partial inhibitory effect.

R domains can be activated directly by accepting a phosphoryl group from acetylphosphate, or by interaction with $BeF_3^-$, a noncovalent mimic of the phosphoryl group, which bonds to an oxygen in the $\beta$-carboxyl group of the aspartate (33, 34). Acetylphosphate had no effect on ACR activity (data not shown), which could be due to phosphatase activity in our membrane preparations. $BeF_3^-$ increased AC activity of wild-type ACR and the D1174A mutant by 10%, whereas it inhibited AC activity in the D1010A mutant by ~30%. This confirms that R1 acts positively and R2 acts negatively on AC activity. However, the D1010A, D1174A, and D1010A/D1174A ACR mutants can all restore the *acr*$^-$ phenotype (Fig. 5*C*), suggesting that regulation of ACR activity by R1 or R2 is of little physiological relevance.

*Role of HisKA Domain*—The results shown in Fig. 5 indicate that cAMP synthesis by ACR does not require the HisC or receiver domains, whereas Fig. 4 shows that ACR activity is only partially dependent on the TM domains. Nevertheless, the ΔTKCR1R2 construct, which contains only the AC domain, has no activity (Fig. 4*B*). The degenerate HisKA domain is the only feature that is absolutely essential for cAMP synthesis. Canonical HisKA domains form intermolecular dimers to allow transphosphorylation by the HisC domains. Although the phosphoryl-accepting histidine is lacking from the

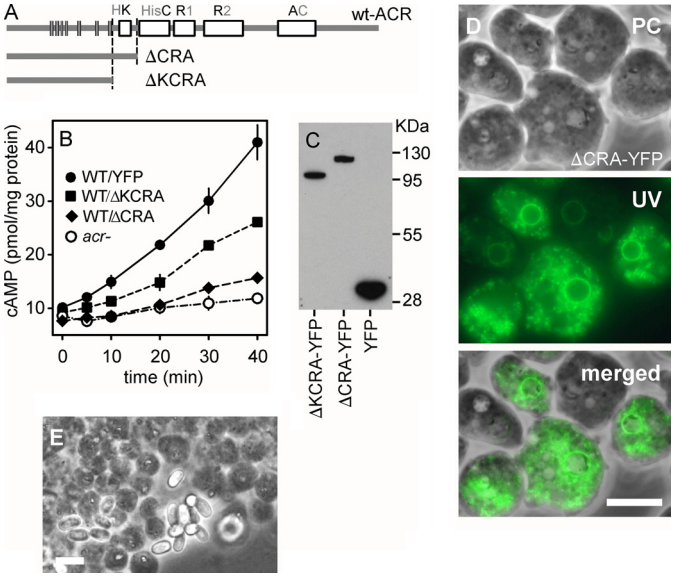


FIGURE 6. **Effects of N-terminal ACR fragments on wild-type ACR activity.** *A*, schematic of ACR constructs that are C-terminally truncated after the HisKA (ΔCRA) or transmembrane domains (ΔKCRA). The fragments were fused to YFP in pB17S-EYFP and transformed into wild-type cells. *B*, lysates of vegetative *acr*$^-$ cells and wild-type cells transformed with ΔCRA-YFP, ΔKCRA-YFP, or empty vector (YFP) were assayed for cAMP synthesis under ACR assay conditions, which was standardized on the total protein content of the lysates. Means and S.E. of three experiments performed in triplicate are shown. *C*, aliquots of 15 $\mu$g of total protein of the transformed wild-type cell lines were subjected to qualitative Western blotting with $\alpha$-GFP antibodies. *D*, visualization of ΔCRA-YFP localization in living vegetative cells by fluorescence and phase contrast microscopy. *E*, squashed spore heads of 2-day-old fruiting bodies of wild-type cells transformed with the ΔCRA-YFP construct contain mainly amoeboid cells. *Scale bar*, 10 $\mu$m. *PC*, phase contrast.

ACR HisKA domain, the $\alpha$-helices that form the intermolecular dimer are present with the first $\alpha$-helix extending up to the seventh TM domain (Fig. 1*B*). Cyclase domains can only be active as dimers with ATP binding and catalysis occurring at the dimer interface. The data therefore suggest that dimerization of the HisKA domains of two ACR molecules acts to facilitate dimerization of their cyclase domains. In that case, a construct that contains the TM and HisKA domains but lacks the cyclase domains should inhibit ACR activity by forming unproductive dimers. Two ACR fragments were prepared that are C-terminally truncated after either the HisKA domain (ΔCRA) or the transmembrane domains (ΔKCRA) (Fig. 6*A*). The constructs were fused to YFP and transformed into wild-type cells. Similar to ACR-YFP, the two truncated proteins also localized to the nuclear membrane and endoplasmic reticulum, as shown for ΔCRA-YFP in Fig. 6*D*. AC activity was measured in wild-type cells transformed either the empty YFP vector or the ΔKCRA-YFP and ΔCRA-YFP constructs, using *acr*$^-$ cells as controls to estimate AC activity due to adenylate cyclase A, adenylate cyclase G, or both. The ΔCRA construct almost completely inhibited endogenous ACR activity (Fig. 6*B*) and also strongly reduced spore encapsulation (Fig. 6*E*). The ΔKCRA construct inhibited endogenous ACR activity by ~40% but did not prevent spore encapsulation (data not shown). The inhibitory effects of both constructs on AC activity suggest that the HisKA domain assisted by the transmembrane domains forms inactive dimers with wild-type ACR.

## DISCUSSION

*ACR Activity Does Not Critically Require Histidine Kinase Activity and Phosphorelay*—Sensor histidine kinase and receiver domains are common intrinsic regulators of many prokaryote adenylate cyclases, but ACR is the only eukaryote adenylate cyclase identified thus far that harbors such features. The results presented in this study indicate that they do not play a critical role in the regulation of cAMP synthesis by ACR or in its established role in spore and stalk cell maturation. ACR activity and its ability to restore the *acr*$^-$ phenotype was unaffected by mutation of three amino acids that are each individually essential for the histidine kinase activity of ACR.

Mutation of the phosphoryl-accepting Asp to Ala in the R1 and R2 receiver domains resulted in 10% inhibition and 2.5-fold stimulation of AC activity, respectively, indicating that phosphorylation of R1 slightly stimulates AC activity, whereas phosphorylation of R2 modestly inhibits activity. $BeF_3^-$, an ion that strongly activates R domains by mimicking Asp phosphorylation, caused only 10% stimulation of AC activity of intact ACR and the R2 phosphorylation mutant. In agreement with the inhibitory effect of R2 phosphorylation, $BeF_3^-$ caused 30% inhibition of AC activity in the R1 phosphorylation mutant. Neither the individual nor the combined mutation of the receiver domains affected the ability of ACR to complement the *acr*$^-$ phenotype (Fig. 5). Evidently, also the receiver domains play only a minor role in controlling ACR activity. This may be related to the fact that both domains have lost the switch pair residues that mediate their phosphorylation-induced conformational change (Fig. 1*C*).

*HisKA Domain Assists Intermolecular Dimerization of Cyclase Domain*—Class III nucleotidyl cyclase domains are active as dimers with the substrate ATP or GTP binding to the dimer interface. However, their intrinsic capacity for dimerization is commonly assisted by interactions between other regions of the protein, such as the double set of six TM helices of mammalian ACs (35), the interaction with dimerizing GCAPs (guanylate cyclase-activating protein) of retinal GCs (36), the dimerizing HAMP (present in histidine kinases, adenyl cyclases, methyl-accepting proteins, and phosphatases) or pH-regulated dimerizing domains of a number of mycobacterial ACs (37), and the extracellular regions of mammalian particulate GCs (38) and *Dictyostelium* ACG (39). Most of the regulation of these enzymes involves processes that reorient the monomers into a configuration that is more favorable for catalysis or that allow the catalytic dimer to form. The catalytic domain of ACR is inactive without the N-terminal histidine kinase and receiver domains. As discussed above, neither histidine kinase activity nor phosphorelay to or from the receiver domains are essential for ACR activity. The need for these domains must therefore depend on another property of their structure.

Sensor histidine kinases are also active as dimers, which are formed by hydrophobic interactions between the two sets of two $\alpha$-helices that make up their HisKA domain (40). This allows transphosphorylation by the attached HATPase-C domain of the His residues that extend from two of the helices.

ACR lacks the conserved His residue, but the conserved HisKA sequence with a set of two helices is present at the location of a canonical HisKA domain. Loss of the HisKA domain rendered ACR inactive, which suggested that the dimerizing HisKA domain was essential for dimerization of the AC domains.

This suggestion was borne out by an experiment showing that an ACR construct that was C-terminally truncated after the HisKA domain inhibited wild-type ACR activity (Fig. 6), most likely by forming unproductive dimers. A construct that harbored only the transmembrane domains partially inhibited ACR activity, suggesting that the transmembrane domains participate in dimer formation. This agrees with the observation that loss of these domains partially reduces the AC activity of otherwise intact ACR (Fig. 4).

In conclusion, it appears that the canonical roles of the sensor histidine kinase and receiver domains have eroded in ACR, leaving only the dimerizing capacity of the HisKA domain as an essential feature of ACR function. The observed conservation of most of the functionally essential residues in the HATPase-C and receiver domains most likely means that these residues are also essential for maintaining protein conformation.

*Acknowledgment—We thank Annette Müller-Taubenberger for the kind gift of calnexin antibody.*

## REFERENCES


1. Linder, J. U., and Schultz, J. E. (2003) *Cellular Signalling* **15,** 1081–1089
2. Ritchie, A. V., van Es, S., Fouquet, C., and Schaap, P. (2008) *Mol. Biol. Evol.* **25,** 2109–2118
3. Baker, D. A., and Kelly, J. M. (2004) *Trends Parasitol.* **20,** 227–232
4. Chen, Y., Cann, M. J., Litvin, T. N., Iourgenko, V., Sinclair, M. L., Levin, L. R., and Buck, J. (2000) *Science* **289,** 625–628
5. Kim, H. J., Chang, W. T., Meima, M., Gross, J. D., and Schaap, P. (1998) *J. Biol. Chem.* **273,** 30859–30862
6. Söderbom, F., Anjard, C., Iranfar, N., Fuller, D., and Loomis, W. F. (1999) *Development* **126,** 5463–5471
7. Aubry, L., and Firtel, R. (1999) *Ann. Rev. Cell. Dev. Biol.* **15,** 469–517
8. Saran, S., Meima, M. E., Alvarez-Curto, E., Weening, K. E., Rozen, D. E., and Schaap, P. (2002) *J. Muscle Res. Cell Motil.* **23,** 793–802
9. Kawabe, Y., Morio, T., James, J. L., Prescott, A. R., Tanaka, Y., and Schaap, P. (2009) *Proc. Natl. Acad. Sci. U.S.A.* **106,** 7089–7094
10. Turner, N. A., Russell, A. D., Furr, J. R., and Lloyd, D. (2000) *J. Antimicrob. Chemother.* **46,** 27–34
11. Marciano-Cabral, F., and Cabral, G. (2003) *Clin. Microbiol. Rev.* **16,** 273–307
12. Gooi, P., Lee-Wing, M., Brownstein, S., El-Defrawy, S., Jackson, W. B., and Mintsioulis, G. (2008) *Cornea* **27,** 246–248
13. Pitt, G. S., Milona, N., Borleis, J., Lin, K. C., Reed, R. R., and Devreotes, P. N. (1992) *Cell* **69,** 305–315
14. Kriebel, P. W., and Parent, C. A. (2004) *IUBMB Life* **56,** 541–546
15. van Es, S., Virdy, K. J., Pitt, G. S., Meima, M., Sands, T. W., Devreotes, P. N., Cotter, D. A., and Schaap, P. (1996) *J. Biol. Chem.* **271,** 23623–23625
16. Alvarez-Curto, E., Saran, S., Meima, M., Zobel, J., Scott, C., and Schaap, P. (2007) *Development* **134,** 959–966
17. Meima, M. E., and Schaap, P. (1999) *Dev. Biol.* **212,** 182–190
18. Kasahara, M., and Ohmori, M. (1999) *J. Biol. Chem.* **274,** 15167–15172
19. Okamoto, S., Kasahara, M., Kamiya, A., Nakahira, Y., and Ohmori, M. (2004) *Photochem. Photobiol.* **80,** 429–433
20. Anjard, C. (2005) in *Dictyostelium Genomics* (Loomis, W. F., and Kuspa, A., eds.) 1st Ed., pp. 59–82, Horizon Bioscience, Norfolk, United Kingdom
21. Shelden, E., and Knecht, D. A. (1995) *J. Cell Sci.* **108,** 1105–1115
22. Faix, J., Kreppel, L., Shaulsky, G., Schleicher, M., and Kimmel, A. R. (2004) *Nucleic Acids Res.* **32,** e143
23. Meima, M. E., Biondi, R. M., and Schaap, P. (2002) *Mol. Biol. Cell* **13,** 3870–3877
24. Müller-Taubenberger, A., Lupas, A. N., Li, H., Ecke, M., Simmeth, E., and Gerisch, G. (2001) *EMBO J.* **20,** 6772–6782
25. Hsing, W., Russo, F. D., Bernd, K. K., and Silhavy, T. J. (1998) *J. Bacteriol.* **180,** 4538–4546
26. Dutta, R., Yoshida, T., and Inouye, M. (2000) *J. Biol. Chem.* **275,** 38645–38653
27. Shabb, J. B. (2001) *Chemical reviews* **101,** 2381–2411
28. West, A. H., and Stock, A. M. (2001) *Trends Biochem. Sci.* **26,** 369–376
29. Hirschman, A., Boukhvalova, M., VanBruggen, R., Wolfe, A. J., and Stewart, R. C. (2001) *Biochemistry* **40,** 13876–13887
30. Stewart, R. C., VanBruggen, R., Ellefson, D. D., and Wolfe, A. J. (1998) *Biochemistry* **37,** 12269–12279
31. Dutta, R., and Inouye, M. (1996) *J. Biol. Chem.* **271,** 1424–1429
32. Gao, R., Mack, T. R., and Stock, A. M. (2007) *Trends Biochem. Sci.* **32,** 225–234
33. Lukat, G. S., McCleary, W. R., Stock, A. M., and Stock, J. B. (1992) *Proc. Natl. Acad. Sci. U.S.A.* **89,** 718–722
34. Yan, D., Cho, H. S., Hastings, C. A., Igo, M. M., Lee, S. Y., Pelton, J. G., Stewart, V., Wemmer, D. E., and Kustu, S. (1999) *Proc. Natl. Acad. Sci. U.S.A.* **96,** 14789–14794
35. Cooper, D. M., and Crossthwaite, A. J. (2006) *Trends Pharmacol. Sci.* **27,** 426–431
36. Olshevskaya, E. V., Ermilov, A. N., and Dizhoor, A. M. (1999) *J. Biol. Chem.* **274,** 25583–25587
37. Linder, J. U., and Schultz, J. E. (2008) *Curr. Opin. Struct. Biol.* **18,** 667–672
38. Misono, K. S., Ogawa, H., Qiu, Y., and Ogata, C. M. (2005) *Peptides* **26,** 957–968
39. Saran, S., and Schaap, P. (2004) *Mol. Biol. Cell* **15,** 1479–1486
40. Bilwes, A. M., Alex, L. A., Crane, B. R., and Simon, M. I. (1999) *Cell* **96,** 131–141
41. McGuffin, L. J., Bryson, K., and Jones, D. T. (2000) *Bioinformatics* **16,** 404–405
42. Tomomori, C., Tanaka, T., Dutta, R., Park, H., Saha, S. K., Zhu, Y., Ishima, R., Liu, D., Tong, K. I., Kurokawa, H., Qian, H., Inouye, M., and Ikura, M. (1999) *Nat. Struct. Biol.* **6,** 729–734
43. Marina, A., Waldburger, C. D., and Hendrickson, W. A. (2005) *EMBO J.* **24,** 4247–4259
44. Tanaka, T., Saha, S. K., Tomomori, C., Ishima, R., Liu, D., Tong, K. I., Park, H., Dutta, R., Qin, L., Swindells, M. B., Yamazaki, T., Ono, A. M., Kainosho, M., Inouye, M., and Ikura, M. (1998) *Nature* **396,** 88–92
45. Bilwes, A. M., Quezada, C. M., Croal, L. R., Crane, B. R., and Simon, M. I. (2001) *Nat. Struct. Biol.* **8,** 353–360
46. Zhu, Y., and Inouye, M. (2002) *Mol. Microbiol.* **45,** 653–663
47. Lee, S. Y., Cho, H. S., Pelton, J. G., Yan, D., Henderson, R. K., King, D. S., Huang, L., Kustu, S., Berry, E. A., and Wemmer, D. E. (2001) *Nat. Struct. Biol.* **8,** 52–56
48. Hastings, C. A., Lee, S. Y., Cho, H. S., Yan, D., Kustu, S., and Wemmer, D. E. (2003) *Biochemistry* **42,** 9081–9090
49. Birck, C., Mourey, L., Gouet, P., Fabry, B., Schumacher, J., Rousseau, P., Kahn, D., and Samama, J. P. (1999) *Structure* **7,** 1505–1515
50. Zhao, X., Copeland, D. M., Soares, A. S., and West, A. H. (2008) *J. Mol. Biol.* **375,** 1141–1151
51. Butler, J. R., and Coukell, M. B. (1992) *Biochem. Cell Biol.* **70,** 169–173